

A Two-Step Geometric Framework For Density Modeling

Sutanoy Dasgupta, Debdeep Pati, and Anuj Srivastava

Department of Statistics, Florida State University

Abstract: We introduce a novel two-step approach for estimating a probability density function (*pdf*) given its samples, with the second and important step coming from a geometric formulation. The procedure involves obtaining an initial estimate of the *pdf* and then transforming it via a warping function to reach the final estimate. The initial estimate is intended to be computationally fast, albeit suboptimal, but its warping creates a larger, flexible class of density functions, resulting in substantially improved estimation. The search for optimal warping is accomplished by mapping diffeomorphic functions to the tangent space of a Hilbert sphere, a vector space whose elements can be expressed using an orthogonal basis. Using a truncated basis expansion, we estimate the optimal warping under a (penalized) likelihood criterion and, thus, the optimal density estimate. This framework is introduced for univariate, unconditional *pdf* estimation and then extended to conditional *pdf* estimation. The approach avoids many of the computational pitfalls associated with classical conditional-density estimation methods, without losing on estimation performance. We derive asymptotic convergence rates of the density estimator and demonstrate this approach using both synthetic datasets and real data, the latter relating to the association of a toxic metabolite on preterm birth.

Key words and phrases: conditional density; density estimation; warped density; Hilbert sphere; sieve estimation; tangent space; weighted likelihood maximization

1. Introduction

Estimating a probability density function (*pdf*) is an important and well studied field of research in statistics. The most basic problem in this area is that of univariate *pdf* estimation from *iid* samples, henceforth referred to as unconditional density estimation. Another problem of significance is conditional density estimation. Here one needs to characterize the behavior of the response variable for different values of the predictors.

Given the importance of *pdf* estimation in statistics and related disciplines, a large number of

solutions have been proposed for each of these problems. While the earliest works focused on parametric solutions, the trend over the last three decades has been to use a nonparametric approach as it minimizes making assumptions about the underlying density (and the relationships between variables for conditional and joint densities). The most common nonparametric techniques are kernel based; please refer to Rosenblatt [1956], Hall et al. [1991], Sheather and Jones [1991], Li and Racine [2007] for a narrative of works. Related to these approaches are “tilting” or “data sharpening” techniques for unconditional density estimation, see for example Hjort and Glad [1995], Doosti and Hall [2016], and the references therein. Kernel methods are very powerful in univariate setting. However, as the number of variables involved gets higher, these methods tend to be computationally inefficient because of the complexities involved in bandwidth selection, especially in conditional density estimation setup.

1.1 Two-Step Approaches for Density Estimation

Another common approach for *pdf* estimation, and the one pursued in the current paper, is a two-step estimation procedure discussed in Leonard [1978], Lenk [1988, 1991], Tokdar et al. [2010], Tokdar [2007], etc. In the first step, one estimates an initial *pdf*, say f_p , from the data, perhaps restricting to a parametric family. Then, in the second step, one *improves* upon this estimate by forming a function $w > 0$, that depends on the initial estimate f_p , and forming a final estimate using $w(x)f_p(x)/\int_y w(y)f_p(y)dy$. Thus, the second step involves estimation of an optimal w in order to estimate the overall *pdf*. In a Bayesian context, the function w is often assigned a Gaussian process prior. While this approach is quite comprehensive, the calculation of the normalization constant makes the computation very cumbersome. The two-step procedures can also be adapted for estimating conditional density functions: first estimate the conditional mean function and then estimate the conditional density of the residuals, as is done in Hansen [2004]. Over the recent years, Bayesian methods for estimating *pdfs* based on mixture models and latent variables have received a lot of attention, primarily due to their excellent practical performances and an increasingly rich set of algorithmic tools for sampling posterior using Markov Chain Monte Carlo (MCMC) methods. References include Escobar and West [1995], Müller et al. [1996], MacEachern and Müller

[1998], Kalli et al. [2011], Jain and Neal [2012], Kundu and Dunson [2014], Bhattacharya et al. [2010] among others. However, these results also come at a very high computational cost typically associated with the MCMC algorithms. Applications of flexible Bayesian models for conditional densities are discussed in MacEachern [1999], De Iorio et al. [2004], Griffin and Steel [2006], Dunson et al. [2007], Chung and Dunson [2009], Norets and Pelenis [2012], among others. Although the literature suggests that such methods based on mixture models have several attractive properties, they lack interpretability and the MCMC solutions for model fitting are overly complicated and expensive.

1.2 A Geometric Two-Step Approach

In this article, we pursue a geometric, two-step approach that is applicable to both conditional and unconditional density estimation. The main motivation here is develop an efficient estimation procedure while retaining good estimation performance. The main difference from the previously described two-step procedure is that the transformation of f_p (in the second step) is now based on the action of a diffeomorphism group, as follows. Let f_p be a strictly positive univariate density on the interval $[0, 1]$; f_p serves as an initial estimate of the *pdf*. Let Γ be the set of all positive diffeomorphisms from $[0, 1]$ to itself, i.e. $\Gamma = \{\gamma | \gamma \text{ is differentiable, } \gamma^{-1} \text{ is differentiable, } \dot{\gamma} > 0, \gamma(0) = 0, \gamma(1) = 1\}$. The elements of Γ play the role of warping functions, or transformations of f_p . Given a $\gamma \in \Gamma$, the transformation of f_p is defined by: $(f_p, \gamma) = (f_p \circ \gamma)\dot{\gamma}$. Henceforth, this transformation is referred to as *warping* of f_p , and the resulting *pdf* f as a *warped density*. This mapping is comprehensive in the sense that one can go from any positive *pdf* to any other positive *pdf* using an appropriate γ . Note that since $\int_0^1 f_p(\gamma(x))\dot{\gamma}(x)dx = 1$, there is no need to normalize this transformation. However, the difficulty of estimating the normalizing constant now shifts to the problem of estimating over Γ and this poses some challenges as Γ is a nonlinear manifold. Note that the use of diffeomorphisms as transformations of a *pdf* have been used in the past, albeit with a different setup and scope; see, for example Saoudi et al. [1994, 1997]. Also, the notion of transformation between *pdfs* has been used in the literature on *optimal transport* as in Tabak and Turner [2013], Tabak and Trigila [2014], with the difference being that the transport is

achieved using an iterated composition of maps and not through an optimization over Γ as done in the current paper. There are two parts to this paper:

1. **Univariate *pdf* Estimation:** We start the paper with a framework for estimating an unconditional, univariate *pdf* defined on $[0, 1]$. This simple setting helps explain and illustrate the main ingredients of the framework. Besides, the proposed geometric framework is naturally univariate in the sense that the transformation defined earlier acts on univariate density shapes, making it a logical starting point for developments. In this simple setup, the approach delivers excellent performance while avoiding heavy computational cost, and is comparable to standard kernel methods, even at very low sample sizes. The framework is then extended to univariate densities with unknown support by scaling the observation domain to $[0, 1]$. A defining characteristic of this warping transformation is that the initial estimate can be constructed in anyway – parametric (e.g. gaussian) or nonparametric (e.g. kernel estimate), and is allowed to be a sub-optimal estimate of the true density.
2. **Conditional Density Estimation:** The second part of the article focuses on extending the framework to estimation of conditional density $f(y|x)$ from $\{(y_i, x_i) : i = 1, \dots, n, y \in \mathbb{R}, x \in \mathbb{R}^d, d \geq 1\}$. The approach is to start with a nonparametric mean regression model of the form $y_i = m(x_i) + \epsilon_i$, $\epsilon_i \sim \mathcal{N}(0, \sigma^2)$, where $m(\cdot)$ is estimated using a standard nonparametric estimator, to obtain an initial conditional density estimate $f_{p,x} \equiv \mathcal{N}(\hat{m}(x), \hat{\sigma}^2)$ at the location x . Then $f_{p,x}$ is warped using a warping function γ_x into a final conditional density estimate. Naturally, the choice of $\gamma_x \in \Gamma$ varies with the predictor x . The selection of γ_x is based on a weighted-likelihood objective function that borrows information from the neighborhood of the location x at which the conditional density is being evaluated.

The main contributions of this paper are as follows:

1. **Avoids Normalizing Constant:** It introduces a geometric approach to two-step estimation, with the second step being based on the action of the diffeomorphism group on the set of positive *pdfs*. This action is chosen so that one does not need a normalization constant, and the resulting estimation process is efficient.

-
2. **Uses Geometry of Γ :** It uses the differential geometry of Γ to map its elements into a subset of a Hilbert space, allowing for a basis expansion and application of standard optimization tools for estimating warping functions.
 3. **Conditional Density Estimation:** It leads to an efficient framework for estimating conditional densities, providing very competitive practical performance and improved computational cost compared to standard kernel techniques.

The rest of this paper is organized as follows. Section 2 outlines the general framework for a univariate unconditional density estimation while Section 3 presents an asymptotic analysis of this estimator. Section 4 contains some simulation study. Section 5 develops theory for conditional density estimation and illustrates properties of the proposed method using simulated datasets. Applications of conditional density estimation using the proposed framework on a real dataset are also presented.

2. Proposed Framework

In this section we develop a two-step framework for estimating univariate, unconditional *pdf*, and start by introducing some notations. Let \mathcal{F} be the set of all strictly positive, univariate probability density functions on $[0, 1]$. Let $p_0 \in \mathcal{F}$ denote the underlying true density and $x_i \sim p_0$, $i = 1, 2, \dots, n$ be independent samples from p_0 . Furthermore, let \mathcal{F}_p be a pre-determined subset of \mathcal{F} , such that an optimal element (based on likelihood or any other desired criterion)) $f_p \in \mathcal{F}_p$ is relatively easy to compute. For instance, any parametric family with a simple maximum-likelihood estimator is a good candidate for f_p . Similarly, kernel density estimates are also good since they are computationally efficient and robust in univariate setups.

Next, we define a warping-based transformation of elements of \mathcal{F}_p , using elements of Γ defined earlier. Note that Γ is an infinite-dimensional manifold that has a group structure under composition as the group operation. That is, for any $\gamma_1, \gamma_2 \in \Gamma$, the composition $\gamma_1 \circ \gamma_2 \in \Gamma$. The identity element of Γ is given by $\gamma_{\text{id}}(t) = t$, and for every $\gamma \in \Gamma$, there is a function $\gamma^{-1} \in \Gamma$ such that $\gamma \circ \gamma^{-1} = \gamma_{\text{id}}$. For any $f_p \in \mathcal{F}_p$ and $\gamma \in \Gamma$, define the mapping $(f_p, \gamma) = (f_p \circ \gamma)\dot{\gamma}$ as given earlier.

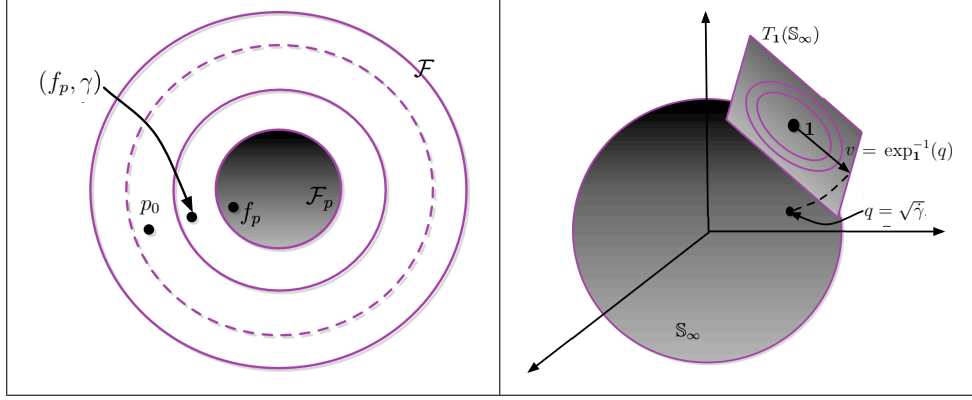


Figure 1: *Left: The true pdf p_0 is estimated by transforming an initial estimate f_p by the warping function γ . The larger the set of allowed γ s, the better the estimate is. Right: Representing warping function γ as element of the tangent space $T_1(\mathbb{S}_\infty^+)$.*

The importance of this mapping comes from the following result.

Proposition 1. *The mapping $\mathcal{F} \times \Gamma \rightarrow \mathcal{F}$, specified above, forms an action of Γ on \mathcal{F} . Furthermore, this action is transitive. In other words, one can reach any element of \mathcal{F} , from any other element of \mathcal{F} using an appropriate element of Γ .*

Proof: We can verify the two properties in the definition of a group action: (1) For any $\gamma_1, \gamma_2 \in \Gamma$ and $f \in \mathcal{F}$, we have $((f, \gamma_1), \gamma_2) = (((f \circ \gamma_1)\dot{\gamma}_1) \circ \gamma_2)\dot{\gamma}_2 = (f, \gamma_1 \circ \gamma_2)$. (2) For any $f \in \mathcal{F}$, $(f, \gamma_{\text{id}}) = f$. To show transitivity, we need to show that given any $f_1, f_2 \in \mathcal{F}$, there exists a $\gamma \in \Gamma$, such that $(f_1, \gamma) = f_2$. If F_1 and F_2 denote the cumulative distribution functions associated with f_1 and f_2 , respectively, then the desired γ is simply $F_1^{-1} \circ F_2$. Since f_1 is strictly positive, F_1^{-1} is well defined and γ is uniquely specified. Furthermore, since f_2 is strictly positive, we have $\dot{\gamma} > 0$ and $\gamma \in \Gamma$. \square

This result implies that together the pair (f_p, γ) spans the full set \mathcal{F} , if γ is chosen freely from Γ . However, if one uses a proper submanifold of Γ , instead of the full Γ , we may not reach the desired p_0 but only approximate it in some way. This intuition is depicted pictorially in the left panel of Figure 1 where the inner disk denotes the set \mathcal{F}_p . The increasing rings around \mathcal{F}_p represent the set $\{(f_p, \gamma) | f_p \in \mathcal{F}_p\}$ with γ belonging to progressively larger dimensional submanifolds of Γ . As the submanifolds approach the full space Γ , the corresponding approximation approaches p_0 .

The submanifolds are introduced formally in the next subsection. More details are also included in Section 6.1(Supplementary Materials).

2.1 Finite-Dimensional Representation of Warping Functions

Given an initial estimate, the focus now shifts to the search for an optimal γ such that the warped density $(f_p \circ \gamma)\dot{\gamma}$ becomes the final estimate under the chosen criterion. However, solving sn optimization over Γ faces two main challenges. First, Γ is a nonlinear manifold, and second, it is infinite-dimensional. We handle the nonlinearity by forming a bijective map from Γ to a tangent space of the unit Hilbert sphere \mathbb{S}_∞ (the tangent space is a vector space), and infinite dimensionality by selecting a finite-dimensional subspace of this tangent space. Together, these two steps are equivalent to finding a family of finite-dimensional submanifolds of Γ that can be *flattened* into vector spaces. This allows for a representation of γ using elements of a Euclidean vector space and an application of standard optimization procedures.

To locally flatten Γ , we define a function $q : [0, 1] \rightarrow \mathbb{R}$, $q(t) = \sqrt{\dot{\gamma}(t)}$, termed the *square-root slope function* (SRSF) of $\gamma \in \Gamma$. (For a discussion on SRSFs of general functions, please refer to Chapter 4 of Srivastava and Klassen [2016]). For any $\gamma \in \Gamma$, its SRSF q is an element of the interior of the positive orthant of the unit Hilbert sphere $\mathbb{S}_\infty \subset \mathbb{L}^2$, denoted by \mathbb{S}_∞^+ . This is because $\|q\|^2 = \int_0^1 q(t)^2 dt = \int_0^1 \dot{\gamma}(t) dt = \gamma(1) - \gamma(0) = 1$. We have a positive orthant, boundaries excluded, because by definition q is a strictly positive function. The mapping between Γ and \mathbb{S}_∞^+ is a bijection, with its inverse given by $\gamma(t) = \int_0^t q(s)^2 ds$. The set \mathbb{S}_∞ is a smooth manifold with known geometry under the \mathbb{L}^2 Riemannian metric Lang [2012]. Although is not a vector space, it can be easily flattened into a vector space (locally) due to its constant curvature. A natural choice for flattening is the vector space tangent to \mathbb{S}_∞^+ at the point $\mathbf{1}$, which a constant function with value 1. ($\mathbf{1}$ is the SRSF corresponding to $\gamma = \gamma_{\text{id}}(t) = t$.) The tangent space of \mathbb{S}_∞^+ at $\mathbf{1}$ is an infinite-dimensional vector space given by: $T_1(\mathbb{S}_\infty^+) = \{v \in \mathbb{L}^2([0, 1], \mathbb{R}) \mid \int_0^1 v(t) dt = \langle v, \mathbf{1} \rangle = 0\}$. See the right panel of Fig. 1 for an illustration of this idea. Next, we define a mapping that takes an arbitrary element of \mathbb{S}_∞^+ to this tangent space. For this *retraction*, we will use the inverse

exponential map; it takes $q \in \mathbb{S}_\infty^+$ to $T_1(\mathbb{S}_\infty^+)$ according to:

$$\exp_1^{-1}(q) : \mathbb{S}_\infty^+ \rightarrow T_1(\mathbb{S}_\infty^+), \quad v = \exp_1^{-1}(q) = \frac{\theta}{\sin(\theta)}(q - \mathbf{1} \cos(\theta)), \quad (2.1)$$

where $\theta = \cos^{-1}(\langle \mathbf{1}, q \rangle)$ is the arc-length from q to $\mathbf{1}$. The right panel of Fig. 1 also shows the mapping from \mathbb{S}_∞^+ to $T_1(\mathbb{S}_\infty^+)$.

We impose a natural Hilbert structure on $T_1(\mathbb{S}_\infty^+)$ using the standard inner product: $\langle v_1, v_2 \rangle = \int_0^1 v_1(t)v_2(t)dt$. It is easy to check that since $q \in \mathbb{S}_\infty^+$, $\theta = \cos^{-1}(\langle \mathbf{1}, q \rangle) < \pi/4$, and hence $\|v\| = \sqrt{\int_0^1 v(t)^2 dt} = \theta < \pi/4$, where $v = \exp_1^{-1}(q)$. Thus, the range of the inverse exponential map is not the entire $T_1(\mathbb{S}_\infty^+)$, but an open subset $T_1^0(\mathbb{S}_\infty^+) = \{v \in T_1(\mathbb{S}_\infty^+) : \|v\| < \pi/4\}$. Further, we can select any orthogonal basis $\mathcal{B} = \{b_j, j = 1, 2, \dots\}$ of the Hilbert space $T_1(\mathbb{S}_\infty^+)$ to express its elements v by their corresponding coefficients; that is, $v(t) = \sum_{j=1}^\infty c_j b_j(t)$, where $c_j = \langle v, b_j \rangle$. The only restriction on the basis elements b_j 's is that they must be orthogonal to $\mathbf{1}$, that is, $\langle b_j, \mathbf{1} \rangle = 0$. In order to map points back from the tangent space to the Hilbert sphere, we use the exponential map, given by:

$$\exp(v) : T_1(\mathbb{S}_\infty^+) \rightarrow \mathbb{S}_\infty, \quad \exp(v) = \cos(\|v\|)\mathbf{1} + \frac{\sin(\|v\|)}{\|v\|} v. \quad (2.2)$$

If we restrict the domain of the exponential map to the subset $T_1^0(\mathbb{S}_\infty^+)$, then the range of this map is \mathbb{S}_∞^+ . Using these two steps, we specify the finite-dimensional, therefore approximate, representation of warping. We define a composite map $H : \Gamma \rightarrow \mathbb{R}^J$, illustrated in Figure 2, as

$$\gamma \in \Gamma \xrightarrow{\text{SRSF}} q = \sqrt{\dot{\gamma}} \in \mathbb{S}_\infty^+ \xrightarrow{\exp_1^{-1}} v \in T_1^0(\mathbb{S}_\infty^+) \xrightarrow{\{b_j\}} \{c_j = \langle v, b_j \rangle\} \in \mathbb{R}^J. \quad (2.3)$$

The range of H is $V_\pi^J = \{c \in \mathbb{R}^J : \|\sum_{j=1}^J c_j b_j\| < \pi/4\} \subset \mathbb{R}^J$. Now, we define $G : \mathbb{R}^J \rightarrow \Gamma$, as

$$\{c_j\} \in \mathbb{R}^J \xrightarrow{\{b_j\}} v = \sum_{j=1}^J c_j b_j \in T_1(\mathbb{S}_\infty^+) \xrightarrow{\exp_1} q = \exp_1(v) \rightarrow \gamma(t) = \int_0^t q(s)^2 ds. \quad (2.4)$$

If we restrict the domain of G to V_π^J , then G is invertible and its inverse is H . Restricting our

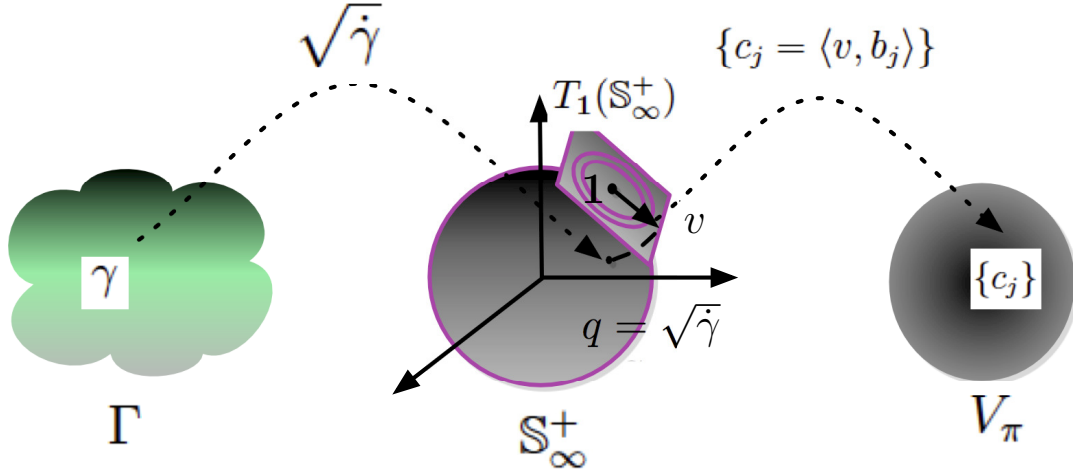


Figure 2: A graphic representation of Eqn. 2.3 leading to a bijective map between Γ and V_π^J .

focus to only the set V_π^J , rather than the entire space \mathbb{R}^J , we identify the function G as H^{-1} . For any $c \in V_\pi^J$, let γ_c denote the diffeomorphism $H^{-1}(c)$. For any fixed J , the set $H^{-1}(V_\pi^J)$ is a J -dimensional submanifold of Γ , and we pose the estimation problem on this submanifold. As J goes to infinity, this submanifold converges to the full group Γ .

With this setting, we can rewrite the estimation of the unknown density p_0 , given an initial estimate f_p , as $\hat{f}(t) = f_p(\gamma_{\hat{c}}(t))\dot{\gamma}_{\hat{c}}(t)$, $t \in [0, 1]$, where $\gamma_{\hat{c}} = H^{-1}(\hat{c})$ and

$$\hat{c} = \operatorname{argmax}_{c \in V_\pi^J} \left(\sum_{i=1}^n \left[\log(f_p(\gamma_c(x_i)) \dot{\gamma}_c(x_i)) \right] \right). \quad (2.5)$$

The truncated basis approximation takes place in the tangent space representation of Γ , rather than in the original space as is the case in Birgé et al. [1998], Donoho et al. [1996] and several others. The tangent space approximation is superior because it is a flat space whereas Γ or \mathbb{S}_∞^+ are not flat.

Choice of Basis Functions: Now that we are in a Hilbert space $T_1(\mathbb{S}_\infty)$, we can choose from a wide range of basis elements. For example, one can use the Fourier basis elements (excluding 1 of course). However, other bases such as splines and Legendre polynomials can also be used. In the experimental studies, we demonstrate an example using the Meyer wavelets that have attractive

properties of infinite differentiability and support over all reals. Vermehren and de Oliveira [2015] provides a closed-form expression for Meyer wavelets and scale function in the time domain, which enables us to use the basis set for representation. However, Meyer wavelets are not naturally orthogonal to 1 and so they need to be orthogonalized first but that can be done offline.

2.2 Advantages Over Direct Approximations

In the previous section, we have used the geometry of Γ to develop a natural, local flattening of Γ . Other, seemingly simpler, choices are also possible but at some cost in estimation performance. For instance, since any γ can also be viewed as a nonnegative function in \mathbb{L}^2 with appropriate constraints, it may be tempting to use $\gamma(t) = \sum_{j=1}^{\infty} c_j b_j(t)$, for some orthogonal basis $\mathcal{B} = \{b_j, j = 1, 2, \dots\}$ of $\mathbb{L}^2[0, 1]$ as in Hothorn et al. [2015]. This seems easier than our approach as it avoids going through a nonlinear transformations. However, the fundamental issue with such an approach is that Γ is a nonlinear manifold and one cannot technically express and estimate elements of Γ directly using linear representations. Hothorn et al. [2015] uses Bernstein polynomials, with monotonically increasing coefficients, to represent elements of Γ . However, one does not reach the entire set Γ using such a representation. To be specific, it is easy to find a significant subset of Γ whose elements cannot be represented in this system. As a simple example, consider a $\gamma = \sum_{i=0}^4 c_i B_{i,4}$ with $c_0 = 0$, $c_1 = 0.4$, $c_2 = 0.3$, $c_3 = 0.5$, $c_4 = 1$ (not satisfying the monotonicity constraint). Here, $B_{i,4}$ refer to the Bernstein basis elements of order 4. Even though this γ is a proper diffeomorphism, it cannot be represented in the system used by Hothorn et al. [2015].

Another issue in directly approximating element of Γ that both γ and $\dot{\gamma}$ are present the final estimate and one needs a good approximation of both of these functions. However, a good approximation of γ does not imply a good approximation of $\dot{\gamma}$. In contrast, the reverse holds true as shown next.

Proposition 2. *For any $\gamma \in \Gamma$, let $\dot{\gamma}_{\text{app}}$ be an approximation of $\dot{\gamma}$, and let γ_{app} be the integral of $\dot{\gamma}_{\text{app}}$. For all $x_0 \in (0, 1]$ consider intervals I_{x_0} of the form $[0, x_0]$. Then, on all intervals I_{x_0} ,*

$$\|\gamma - \gamma_{\text{app}}\|_{\infty} \leq \|\dot{\gamma} - \dot{\gamma}_{\text{app}}\|_{\infty}.$$

Proof: Let $t \in I_{x_0}$. $|\gamma(t) - \gamma_{\text{app}}(t)| = |\int_0^t \dot{\gamma}(s)ds - \int_0^t \dot{\gamma}_{\text{app}}(s)ds| \leq \int_0^t |\dot{\gamma}(s) - \dot{\gamma}_{\text{app}}(s)|ds \leq \|\dot{\gamma} - \dot{\gamma}_{\text{app}}\|_{\infty} \cdot t \leq \|\dot{\gamma} - \dot{\gamma}_{\text{app}}\|_{\infty} \cdot x_0 \leq \|\dot{\gamma} - \dot{\gamma}_{\text{app}}\|_{\infty} \square$ This proposition states that a good approximation of $\dot{\gamma}$ ensures a good approximation of γ , and supports our approach of approximating γ via the inverse exponential transformation of its SRSF to the tangent space $T_1(\mathbb{S}_{\infty}^+)$. On the other hand, a direct approximation of γ will need many more basis elements to ensure a good approximation of $\dot{\gamma}$.

2.3 Estimation of Densities with Unknown Support

So far we have restricted to the interval $[0, 1]$ for representing a *pdf*. However, the framework extends naturally to *pdfs* with unknown support. For that, we simply scale the observations to $[0, 1]$ and carry out the original procedure. Let $X_1, X_2, \dots, X_n \sim p_0$, where X_i s are n independent observations from a density p_0 with an unknown support. We transform the data as $Y_i = \frac{X_i - A}{B - A}$, where A and B are the estimated boundaries of the density. Following Turnbull and Ghosh [2014], we take $A = X_{(1)} - s_X/\sqrt{n}$, and $B = X_{(n)} + s_X/\sqrt{n}$, where $X_{(1)}$ and $X_{(n)}$ are the first and last order statistics of X , and s_X is the sample standard deviation of the observed samples. Using the scaled data, we can find the estimated *pdf* f_w on $[0, 1]$ and then undo the scaling to reach the final solution. Turnbull and Ghosh [2014] provide a justification for the choice of A and B as the estimates for the bounds of the density. They also discuss an alternate way of estimating the boundaries using ideas presented in De Carvalho [2011], and suggest that the Carvalho method produces wider and more conservative boundary estimates.

Finally, using the fact that any piecewise continuous density function, with support \mathbb{R} and range $\mathbb{R}_{\geq 0}$, can be approximated to any desired degree by a strictly positive density function on some bounded interval $[A, B]$ (under \mathbb{L}^2 norm, for example), we can extend our method to this larger class of functions.

3. Asymptotic Analysis and Convergence Rate Bounds

We have represented an arbitrary *pdf* as a function of the coefficients *w.r.t* a basis set of the tangent space. We note that in order to represent the entire space \mathcal{F} , we need a Hilbert basis with infinitely many elements. However, in practice, we use only a finite number J of basis elements. Hence, we are actually optimizing over a subset of the space of density functions based on only a few basis elements and using it to approximate the true density. This subset is called the *approximating space*. Since we are performing maximum likelihood estimation over an approximating space for *pdfs*, our estimation is akin to the sieve MLE, discussed in Wong and Shen [1995].

First, we introduce some notations. Recall that \mathcal{F} is the space of all univariate, strictly positive *pdfs* on $[0, 1]$ and zero elsewhere. Let \mathcal{F}_n be the approximating space of \mathcal{F} when using $J = k_n$ basis elements for the tangent space $T_1(\mathbb{S}_\infty^+)$, where k_n is some function of the number of observations n . Let $f_p \in \mathcal{F}_p \subset \mathcal{F}$ be an initial estimate, and let $\mathcal{F}_n = \{f_p(\gamma)\dot{\gamma}, \gamma = H^{-1}(c) \mid c \in V_\pi^J \subset \mathbb{R}^{k_n}\}$, where H and V_π^J are defined in Section 2.1. As $n \rightarrow \infty, k_n \rightarrow \infty$. So $\mathcal{F}_n \rightarrow \mathcal{F}$ as $n \rightarrow \infty$. Let η_n be a sequence of positive numbers converging to 0. Let $\mathcal{Y}^{(n)}$ be the space of n observed points. We call an estimator $\hat{p} : \mathcal{Y}^{(n)} \rightarrow \mathcal{F}_n$ an η_n sieve MLE if

$$\frac{1}{n} \sum_{i=1}^n \log \hat{p}(Y_i) \geq \sup_{p \in \mathcal{F}_n} \frac{1}{n} \sum_{i=1}^n \log p(Y_i) - \eta_n$$

In the proposed method, the estimated *pdf* is exactly $\sup_{p \in \mathcal{F}_n} \frac{1}{n} \sum_{i=1}^n \log p(Y_i)$. Therefore, this estimate is a sieve MLE with $\eta_n \equiv 0$. Let p_0 denote the true density which is assumed to belong a Hölder space of order $\beta > 0$. By the equivalence of the pdf space and the coefficient space of expansion of γ (refer to Appendix S1.1), it is straightforward to show that if $k_n = l_1 n^{1/(2\beta+1)}$ then $\inf_{f \in \mathcal{F}_n} \|p_0 - f\|_\infty \leq l_2 n^{-\beta/(2\beta+1)}$ for some arbitrary constants l_1 and l_2 . This follows from standard approximation results in \mathbb{L}^2 basis (e.g. Fourier) of Hölder functions of order β . For a detailed discussion please refer to Triebel [2006].

To control the approximation error, Wong and Shen [1995] introduces a family of discrepancies. They define $\delta_n(p_0, \mathcal{F}_n) = \inf_{f \in \mathcal{F}_n} \rho(p_0, f)$, called the ρ -approximation error at p_0 . The control of

the approximation error of \mathcal{F}_n at p_0 is necessary for obtaining results on the convergence rate for sieve MLEs. We follow Wong and Shen [1995] to introduce a family of indexes of discrepancy in order to formulate the condition on the approximation error of \mathcal{F}_n . Let

$$g_\alpha(x) = \begin{cases} (1/\alpha)[x^\alpha - 1], & -1 < \alpha < 0 \text{ or } 0 < \alpha \leq 1 \\ \log x, & \text{if } \alpha = 0+ \end{cases}$$

Set $x = p/f$ and define $\rho_\alpha(p, f) = E_p g_\alpha(X) = \int p g_\alpha(p/f)$. We define $\delta_n(\alpha) = \inf_{f \in \mathcal{F}_n} \rho_\alpha(p_0, f)$. We use $\alpha = 1$ for our results. Then $\delta_n(1) = \int (p_0 - f)^2 / f$.

The δ -cover of a set T wrt a metric ρ is a set $\{\Theta^1, \dots, \Theta^N\} \subset T$ such that for each $\Theta \in T$, there exists some $i \in \{1, \dots, N\}$ with $\rho(\Theta, \Theta_i) \leq \delta$. The covering number N is the cardinality of the smallest delta cover. Then $\log(N)$ is the metric entropy for T . The following Lemma provides a bound for the Hellinger metric entropy for \mathcal{F}_n .

Lemma 1. *There exists positive constants C_3 and C_4 and a positive $\epsilon < 1$ such that,*

$$\int_{\epsilon^2/2^8}^{\sqrt{2}\epsilon} H^{1/2}\left(\frac{u}{C_3}, \mathcal{F}_n\right) du \leq C_4 n^{1/2} \epsilon^2, \quad (3.1)$$

The following corollary provides a uniform exponential bound on likelihood ratio surfaces and follows from Lemma 1 due to Theorem 1 of Wong and Shen [1995].

Corollary 1. *If Lemma 1 holds, there exists positive constants C_1 and C_2 such that for any $\epsilon > 0$,*

$$P^* \left(\sup_{\{\|p^{1/2} - p_0^{1/2}\|_2 \geq \epsilon, p \in \mathcal{F}_n\}} \prod_{i=1}^n p(Y_i)/p_0(Y_i) \geq \exp(-C_1 n \epsilon^2) \right) \leq 4 \exp(-C_2 n \epsilon^2)$$

Lemma 2. *There exists a positive constant C_5 such that $\delta_n(1) = C_5 n^{-2\beta/(2\beta+1)}$.*

The following theorem provides convergence rates of the sieve estimators.

Theorem 1. *Under the assumptions listed above, let C_1, \dots, C_4 , be as in Lemma 1 and Corollary*

1. Define, $\epsilon_n^* = Mn^{-\beta/(2\beta+1)}\sqrt{\log n}$ for some $M > 0$. Then if $\delta_n(1) < 1$,

$$P(\|q^{1/2} - p_0^{1/2}\|_2 \geq \epsilon_n^*) \leq 5\exp(-C_2n(\epsilon_n^*)^2) + \exp(-\frac{1}{4}n\alpha C_1(\epsilon_n^*)^2). \quad (3.2)$$

The proofs of the results are deferred to Section 6 (Supplementary Materials). Note that the convergence rate is independent of the initial step f_p (upto constant terms) because the estimation problem is shifted to Γ given a fixed choice of f_p .

4. Simulation Studies

Next, we present results from experiments on univariate unconditional density estimation procedure involving two simulated datasets. The computations described here are performed on an Intel(R) Core(TM) i7-3610QM CPU processor laptop, and the computational times are reported for each experiment. We compare the proposed solution with two standard techniques: (1) kernel density estimates with bandwidth selected by unbiased cross validation method, henceforth referred to as *kernel(ucv)*, (2) a standard Bayesian technique using the function *DPdensity* in the R package *DPPackage*. We focus on the average performance of the different techniques over 100 independent samples from the true density. We use *ksdensity* as the initial estimate f_p for our approach. We consider sample sizes of 25, 100 and 1000, to study the effect of n on estimation performance and computational cost. The performance is evaluated using multiple norms: \mathbb{L}^2 , \mathbb{L}^1 norm and \mathbb{L}^∞ norm, averaged over the 100 samples.

We borrow the first example from Tokdar [2007] and Lenk [1991], where $p_0 \propto 0.75\exp(\text{rate} = 3) + 0.25\mathcal{N}(0.75, 2^2)$, a mixture of exponential and normal density truncated to the interval $[0, 1]$: Table 1 summarizes estimation performance and computation cost for these methods at different sample sizes. The values of mean and standard deviation have been scaled by 100 for convenience. It is observed that when $n = 25$, *kernel(ucv)* method outperforms the other two methods. However, for higher sample sizes, the warping-based method has a better overall performance. The computational cost of the proposed method, while higher than *kernel(ucv)*, is much less than the *DPdensity* for higher sample sizes. In this example, we also studied performance using the Fourier

Table 1: A comparison of the performances for mixture of exponential and normal example.

Method:		DPDensity			Kernel(ucv)			Warped Estimate		
n	Norm	Mean	std.dev.	Time	Mean	std.dev	Time	Mean	std.dev	Time
25	\mathbb{L}^1	37.26	8.63		33.51	11.97		39.53	9.8	
	\mathbb{L}^2	5.05	0.9	4 sec	4.5	1.44	< 1 sec	4.96	1.27	5 sec
	\mathbb{L}^∞	1.64	0.21		1.44	0.47		1.34	0.53	
100	\mathbb{L}^1	22.87	5.32		21.9	5.54		22.46	4.95	
	\mathbb{L}^2	3.47	0.58	18 sec	3.14	0.57	< 1 sec	2.93	0.61	5 sec
	\mathbb{L}^∞	1.49	0.2		1.23	0.24		0.88	0.34	
1000	\mathbb{L}^1	10.79	2.05		11.57	2.14		10.05	1.36	
	\mathbb{L}^2	1.83	0.24	225 sec	1.67	0.23	< 1 sec	1.31	0.16	5 sec
	\mathbb{L}^∞	1.18	0.2		0.88	0.22		0.5	0.17	

Table 2: Comparison for claw density example.

Method:		DPDensity			Kernel(ucv)			Warped Estimate		
n	Norm	Mean	std.dev.	Time	Mean	std.dev	Time	Mean	std.dev	Time
25	\mathbb{L}^1	39.15	6.29		17.06	2.33		18.28	3.3	
	\mathbb{L}^2	5.46	0.48	4 sec	2.09	0.3	1 sec	2.41	0.43	105 sec
	\mathbb{L}^∞	1.2	0.05		0.5	0.14		0.64	0.17	
100	\mathbb{L}^1	28.39	4.55		8.54	2.38		9.06	2.6	
	\mathbb{L}^2	4.31	0.46	26 sec	1.18	0.28	1 sec	1.3	0.35	85 sec
	\mathbb{L}^∞	1.08	0.09		0.34	0.08		0.42	0.13	
1000	\mathbb{L}^1	19.28	1.63		2.4	0.38		2.46	0.43	
	\mathbb{L}^2	3.16	0.15	331 sec	0.38	0.06	1 sec	0.4	0.08	71 sec
	\mathbb{L}^∞	0.83	0.04		0.14	0.03		0.15	0.04	

basis and the results were very similar.

For the second example we take Example 10 from Marron and Wand [1992], which uses a claw density: $p_0 = \frac{1}{2}\mathcal{N}(0, 1) + \sum_{l=0}^4 \frac{1}{10}\mathcal{N}(\frac{l}{2} - 1, (0.1)^2)$.

Unlike the previous example, instead of fixing J , the number of tangent basis elements, we employ Algorithm 1 (please refer to Section 7 of the Supplementary Materials) to find the optimal J based on the AIC, with a maximum allowed value of 40 basis elements. Consequently, as can be seen in Table 2, the computation cost goes up. Additionally, we note that the cost is highest for $n = 25$ and actually decreases as n increases. This is because for small n there is less information and it take more time for the objective function to converge.

Table 2 shows that at $n = 1000$, the performances of all three methods are similar, especially

between $kernel(ucv)$ and warped density estimate. In fact, the warped density estimate and $kernel(ucv)$ perform similarly even at low sample sizes, while $DPdensity$ performs poorly. These results were obtained using the Fourier basis but the results for Meyer basis were similar.

5. Extension to Conditional Density Estimation

The idea of using diffeomorphisms to warp an initial density estimate, while maximizing likelihood, extends naturally to conditional density estimation. Consider the following setup: Let X be a fixed d -dimensional random variable with a positive density on its support. Let $Y \sim p_0(m(X), \sigma_X^2)$, where p_0 is the unknown conditional density that changes smoothly with X ; $m(X)$ is the unknown mean function, assumed to be differentiable; and, σ_X^2 is the unknown variance, which may or may not depend on X . Y is assumed to have a univariate, continuous distribution with support on unknown interval $[A, B]$. We observe the pairs $(Y_i, X_i), i = 1, \dots, n$, and are interested in recovering the conditional density $p_0(m(X), \sigma_X^2)$.

In order to initialize estimation, we assume a nonparametric mean regression model of the form $y_i = m(x_i) + \epsilon_i$, $\epsilon_i \sim f_p(0, \sigma^2)$, where $m(\cdot)$ is estimated using standard local linear regression, f_p is an initial estimate for the conditional density of the response variable, and σ^2 is estimated using the sample standard deviation of the residuals $Y_i - \hat{m}(X_i)$. We have used truncated normal density as f_p in the experiments presented later but other choices are equally valid. As was the case in unconditional pdf estimation, it is not required that the initial estimate has mean function close to the true mean function, or assume any particular form. The only requirement is that the initial conditional density should be continuous and bounded away from zero, and the density should vary smoothly with X in the sense that if X_1 and X_2 are close to each other, then $f_p(Y|X_1)$ should be close to $f_p(Y|X_2)$ in the \mathbb{L}^2 or some other metric. Let F_{p,x_0} be the corresponding initial estimate of the conditional distribution function of Y , given $X = x_0$ for some given value of the predictor x_0 . Then, the warped density estimate, for a warping function γ and location x_0 , is $f_{w,x_0}(y|X = x_0) = f_p(\gamma(y), \hat{m}(x_0), \hat{\sigma}^2)\dot{\gamma}(y)$. If F_{t,x_0} is the true conditional distribution function of Y , given $X = x_0$, then the true γ at location x_0 is $\gamma_{x_0} = F_{p,x_0}^{-1} \circ F_{t,x_0}$. Setting

$f_{p,x_0} \equiv f_p(\hat{m}(X), \hat{\sigma}^2)$, we estimate the optimal γ by a weighted maximum likelihood estimation: $\hat{\gamma}_{x_0} = \operatorname{argmax}_{\gamma \in \Gamma} \left(\sum_{i=1}^n \log \left[(f_{p,x_0}(\gamma(y_i)|x_i)\dot{\gamma}) W_{x_0,i} \right] \right)$, where $W_{x_0,i}$ is the localized weight associated with the i th observation, calculated as:

$$W_{x_0,i} = \frac{\mathcal{N}(\|X_i - x_0\|_2/h(x_0); 0, 1)}{\sum_{j=1}^n \mathcal{N}(\|X_j - x_0\|_2/h(x_0); 0, 1)}$$

where $\mathcal{N}(\cdot; 0, 1)$ is the standard normal *pdf* and $h(x_0)$ is the parameter that controls the relative weights associated with the observations. However, weights defined in this way results in higher bias because information is being borrowed from all observations. As discussed in an example in Bashtannyk and Hyndman [2001], we allow only a specified fraction of the observations X_i to have a positive weight. However, using too small a fraction will result in unstable estimates and poor practical performance because the effective sample size will be too small. Hence we advocate using the nearest 50% of the observations (nearest to the target location) for borrowing information and then calculating the weights for this smaller sample as defined before.

The parameter $h(x_0)$ is akin to the bandwidth parameter associated with traditional kernel methods for density estimation. A very large value of $h(x_0)$ distributes approximately equal weight to all the observations, whereas a very small value considers only the observations in a small neighborhood around x_0 . Since $h(x_0)$ is scalar, the tremendous computational cost associated with obtaining cross-validated bandwidths in each predictor dimension, when the predictor dimension is high, is avoided. When the predictor is one-dimensional, the parameter $h(x_0)$ is chosen according to the location x_0 using a two-step procedure as follows:

1. Compute a standard kernel density estimate \hat{K} of the predictor space using a fixed bandwidth chosen according to any standard criterion. Let h be the fixed bandwidth used.
2. Then, set the bandwidth parameter $h(x_0)$ at location x_0 to be $h(x_0) = h/\sqrt{\hat{K}(x_0)}$.

The intuition is that h controls the overall smoothing of the predictor space based on the sample points, and the $\sqrt{\hat{K}(x_0)}$ stretches or shrinks the bandwidth at the particular location. The choice of the adaptive bandwidth parameter is motivated from the variable bandwidth kernel density es-

timators discussed in Terrell and Scott [1992], Van Kerm [2003] and Abramson [1982], among others. In case of d independent predictors, $h(\mathbf{x}_0)$ at \mathbf{x}_0 is chosen as follows:

1. Compute the kernel density estimate $\hat{K}_i, i \in 1, \dots, d$ for the d predictors with associated bandwidths h_1, h_2, \dots, h_d . Then h is chosen as the harmonic mean of the h_i 's.
2. Once h is obtained, the bandwidth parameter $h(\mathbf{x}_0)$ at \mathbf{x}_0 is given by:

$$h(\mathbf{x}_0) = h / \left(\prod_{i=1}^d \sqrt{\hat{K}_i(x_{0i})} \right) \quad (5.1)$$

where x_{0i} is the i th coordinate of \mathbf{x}_0 .

This choice of using the harmonic mean is based on the dependence of the minimax rates of convergence of estimators to the harmonic mean of the smoothness of the density along the different dimensions, as discussed in Lepski [2015].

5.1 Simulation Studies

We present two examples to illustrate the proposed method and compare it with a standard R package NP (with kd-tree package implementation to reduce computation time). In these experiments we have used a gaussian family for f_p , the initial parametric conditional density estimate. To estimate the mean function, we have used a local-linear regression function with gaussian kernel weights and bandwidth obtained from `kernel(bcv)` available in R package `kedd`. Bandwidth from other estimators like unbiased cross validation and even the naive *ksdensity* function in MATLAB produce practically identical results. We use six basis elements for the tangent space representation throughout.

For comparison, we used 100 samples each of size $n = 100$ and $n = 1000$ to obtain a mean integrated squared-error loss function estimate, a mean absolute error estimate and a mean \mathbb{L}^∞ loss function estimate from the densities evaluated over a grid of 100 points at 10 equidistant locations over the support of each of the predictors. As a first example, we consider a situation where the true conditional density is a Laplace distribution, i.e. $f(y_i | X = x_i) =$

Table 3: A comparison of the performances NP package and Warped estimate for simulated examples.

Method:			NP package			Warped Estimate		
Example	n	Norm	Mean	std.dev	Time	Mean	std.dev	Time
Example 1	100	\mathbb{L}^1	4.11	0.51		3.28	0.44	
		ISE	0.59	0.12	1 sec	0.41	0.11	1 sec
		\mathbb{L}^∞	0.40	0.07		0.88	0.34	
	1000	\mathbb{L}^1	2.50	0.24		2.46	0.11	
		ISE	0.26	0.04	51 sec	0.25	0.03	3 sec
		\mathbb{L}^∞	0.39	0.06		0.36	0.04	
Example 2	100	\mathbb{L}^1	60.49	6.67		58.55	5.28	
		ISE	11.43	4.01	2 sec	10.38	1.82	2 sec
		\mathbb{L}^∞	2.47	0.43		2.41	0.35	
	1000	\mathbb{L}^1	42.10	4.32		53.53	1.86	
		ISE	5.88	1.41	198 sec	8.96	0.57	7 sec
		\mathbb{L}^∞	2.38	0.29		2.24	0.25	

$D\text{Exp}(y_i; \text{mean}=(2x_i - 1), \text{var}=1)$ and $X_i \sim \mathcal{N}(0, 1)$. As the second example we take a bi-variate predictor scenario where $f(y_i|X = (x_{1i}, x_{2i})) = (1 - e^{-x_{2i}})\mathcal{N}(y_i; (x_{1i} + 2), (0.5)^2) + (e^{-x_{2i}})D\text{Exp}(y_i; (x_{1i} - 1), 1)$ and the predictors $X_1 \sim 0.95\mathcal{N}(0, (0.4)^2) + 0.05\mathcal{N}(0, (1.4)^2)$ and $X_2 \sim \mathbb{U}(0, 1)$.

The results are summarized in Table 3. From the results it is clear that when the sample size is low the performance of the warped estimate is better and more stable. When the sample size is high the performance of the two methods are more comparable though the warped estimation method still provides more stable performances. However, the computation cost of the NP package is very high even with the kd-tree implementation, whereas the warped estimation is computationally very efficient.

5.2 Application to Epidemiology

Longnecker et al. [2001] studied the association of DDT metabolite DDE exposure and preterm birth in a study based on the US Collaborative Perinatal Project (CPP). DDT is very effective against malaria inflicting mosquitoes and hence is frequently used in malaria-endemic areas in spite of evidence that suggests associated health risks. Both Longnecker et al. [2001] and Dunson

and Park [2008] concluded that higher levels of DDE exposure is associated with higher risks of preterm birth. The response variable in question is the gestational age at delivery (GAD), and deliveries occurring prior to 37 weeks of gestation is considered as preterm. Longnecker et al. [2001] also recorded the serum triglycerine level, among several other factors, and included it in their model since serum DDE level can be affected by concentration of serum lipids.

We study the Longnecker data to investigate the effect of varying levels of DDE on the distribution of GAD, focusing on the left tail of distribution to assess the effect on preterm births. In our study, following Dunson and Park [2008], we include only the 2313 subjects for whom the gestation age at delivery is less than 45 weeks, attributing higher values to measurement errors. We study the conditional density of GAD given different doses of DDE in the serum. We also study the effect of different levels of triglyceride on GAD. However, since DDE is a possible confounding factor, we conduct a bivariate analysis, including both DDE dose and triglyceride level as the covariates and study the effect on GAD at varying levels of one covariate, keeping the other fixed. We also investigate whether different levels of one covariate affect the distribution of the other.

Based on our findings, the very erratic behavior at locations where the DDE dose or triglyceride levels are 99th percentile is seen with some skepticism because of the sparsity of the data in that region. We notice an increasingly prominent peak near the left tail of GAD distribution with increasing dose of DDE, which agrees with the results of Longnecker et al. [2001] and Dunson and Park [2008], shown in the left panel of Figure 3. The right panel of Figure 3 suggests a tendency of higher risks of preterm birth at higher doses of triglycerides as well, though the difference was less pronounced.

To investigate whether the results corresponding to triglycerides were confounded by the DDE doses, we first study the effect of triglyceride levels on DDE distribution and vice versa. Figure 4 shows that the distributions of the covariates are completely identical for varying levels of the other. The only exception is at 99th percentile of triglyceride for which the distribution of DDE doses seem to be shifted to the right. For fixed levels of triglyceride, increasing DDE doses shows an increasing left peak except where both DDE and triglyceride levels are very high, shown in Figure 5. For fixed doses of DDE the distribution of GAD at different levels of triglyceride do not follow

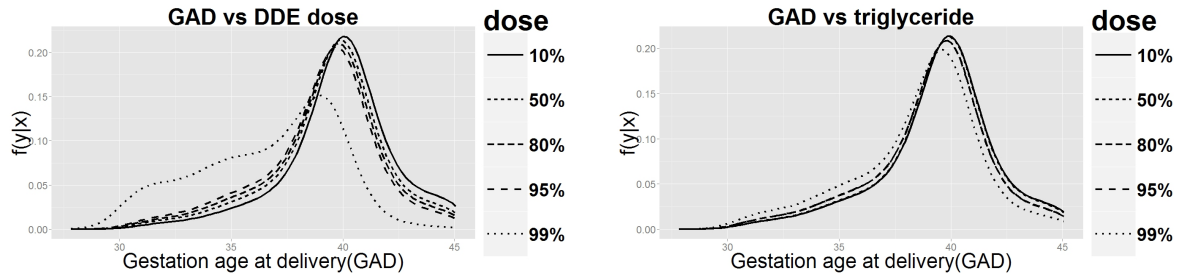


Figure 3: *Distribution of gestation age at delivery for varying levels of DDE and triglyceride*

any increasing trend and are almost indistinguishable from each other for all the different doses of DDE, as seen in Figure 6. This suggests that the increased risk of preterm birth can be attributed primarily to DDE doses, and there is no significant effect of different triglyceride levels on the gestation age. The apparent increasing risk of preterm birth for increasing level of triglycerides seen in the right panel of Figure 3 is mainly caused by DDE doses acting as a confounding factor.

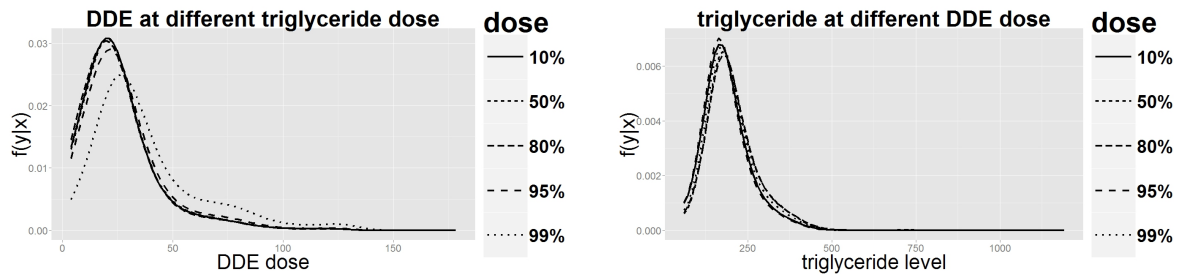


Figure 4: *Distribution of DDE and triglyceride at different levels of the other*

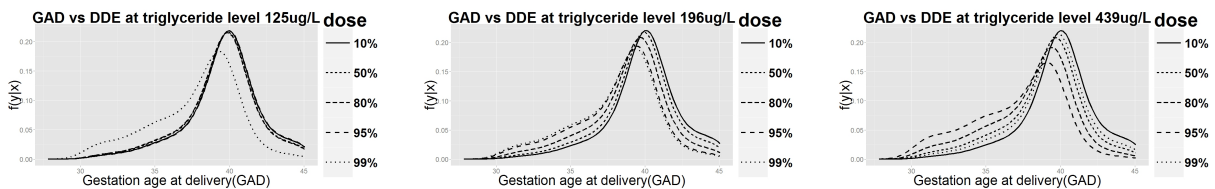


Figure 5: *Distribution of gestation at varying levels of DDE for fixed values of triglyceride*

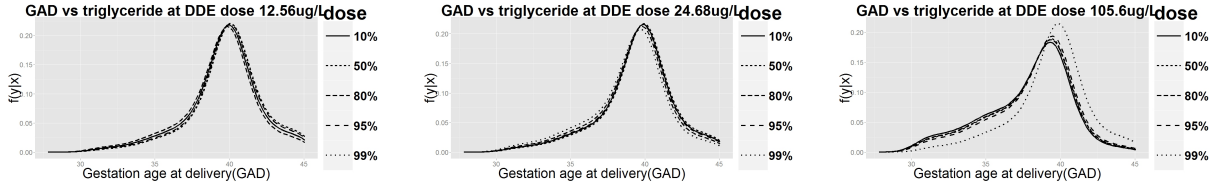


Figure 6: *Distribution of gestation at varying levels of triglyceride for fixed values of DDE*

SUPPLEMENTARY MATERIALS

6. Theoretical Results

Let \mathcal{F} and \mathcal{F}_n be as defined in Section 2 of the manuscript. To control the approximation error of \mathcal{F}_n , Wong and Shen [1995] introduces a family of discrepancies. They define $\delta_n(p_0, \mathcal{F}_n) = \inf_{f \in \mathcal{F}_n} \rho(p_0, f)$, called the ρ -approximation error at p_0 . Here p_0 is the true density which is assumed to belong to Hölder space of order $\beta > 0$ so that if $k_n = l_1 n^{1/(2\beta+1)}$ then $\inf_{f \in \mathcal{F}_n} \|p_0 - f\|_\infty \leq l_2 n^{-\beta/(2\beta+1)}$ for some arbitrary constants l_1 and l_2 . The control of the approximation error of \mathcal{F}_n at p_0 is necessary for obtaining results on the convergence rate for sieve MLEs. We follow Wong and Shen [1995] to introduce a family of indexes of discrepancy in order to formulate the condition on the approximation error of \mathcal{F}_n . Let

$$g_\alpha(x) = \begin{cases} (1/\alpha)[x^\alpha - 1], & -1 < \alpha < 0 \text{ or } 0 < \alpha \leq 1 \\ \log x, & \text{if } \alpha = 0+ \end{cases}$$

Set $x = p/f$ and define $\rho_\alpha(p, f) = E_p g_\alpha(X) = \int p g_\alpha(p/f)$. We define $\delta_n(\alpha) = \inf_{f \in \mathcal{F}_n} \rho_\alpha(p_0, f)$. We call a finite set $\{(f_j^L, f_j^U), j = 1, \dots, N\}$ a Hellinger u -bracketing of \mathcal{F}_n if $\|f_j^{L1/2} - f_j^{U1/2}\|_2 \leq u$ for $j = 1, \dots, N$, and for any $p \in \mathcal{F}_n$, there is a j such that $f_j^L \leq p \leq f_j^U$. Let $H(u, \mathcal{F}_n)$ be the Hellinger metric entropy of \mathcal{F}_n , defined as the cardinality of the u -bracketing of \mathcal{F}_n of the smallest size. Let f_p be the initial estimate on which we use the group action of the space of diffeomorphisms to arrive at the final estimate. Throughout, c_1 and c_2 have been used to represent coefficient vectors in the tangent space of the Hilbert sphere for some fixed basis set corresponding

to warping function that acts on f_p . When c_1 denotes the coefficient vector corresponding to the true density denoted by $p_0 \in \mathcal{F}$ and c_2 corresponds to the estimate $f \in \mathcal{F}_n$, $c_1^{>k_n}$ represents the $(k_n + 1)$ th onwards coordinates of c_1 . l_1, l_2, l_3 and l_4 are used to indicate specific constants. Also, M_1, M_2, M_3, \dots , have been used to represent generic constants whose value can change from step to step but is independent of other terms in the expressions.

6.1 pdf space versus the coefficient space

Let f_1 and f_2 be two pdfs on \mathcal{F}_n with corresponding cumulative distribution functions F_1 and F_2 . Let f_p be the initial density estimate on \mathcal{F}_p such that f_p is strictly positive and Lipschitz continuous with cumulative distribution function F_p . Let $\gamma_1 = F_p^{-1} \circ F_1$ and $\gamma_2 = F_p^{-1} \circ F_2$. Let $c_1 = (c_{11}, \dots, c_{1k_n})^T$ and $c_2 = (c_{21}, \dots, c_{2k_n})^T$ be the coefficients associated with the two elements of $T_1(\mathbb{S}_\infty)$ corresponding to the tangent space representation of γ_1 and γ_2 . Here \mathcal{F}_n and k_n are as introduced in section 2 of the manuscript. Then the following Lemma bounds the norm difference of f_1 and f_2 with the norm difference in the coefficients.

Proposition 3. $|f_1 - f_2| \leq M_0 \|c_1 - c_2\|_1$ where $M_0 > 0$ is a constant.

Proof. Let c_1 and c_2 be the coefficients associated with two elements v_1 and v_2 of $T_1(\mathbb{S}_\infty)$, defined in Section 2 of the manuscript and let q_1 and q_2 represent the corresponding elements on the Hilbert sphere. Then there exists $M_1 \in \mathbb{R}$ such that $|B_i| < M_1$, where B_i is the i th basis function, $i = 1, 2, \dots, k_n$. Let $v_1 = \sum_{i=1}^{k_n} c_{1i} B_i$, $v_2 = \sum_{i=1}^{k_n} c_{2i} B_i$. Then $v_1, v_2 \in T_1(\mathbb{S}_\infty)$ with $\|v_1\| < \pi/4$ and $\|v_2\| < \pi/4$. Hence we have

$$(v_1 - v_2)(t) = \sum_{i=1}^{k_n} (c_{1i} - c_{2i}) B_i(t) < M_1 \sum_{i=1}^{k_n} |c_{1i} - c_{2i}| = M_1 \|c_1 - c_2\|_1$$

$$\|v_1 - v_2\| = \sqrt{\int_0^1 (v_1 - v_2)^T (v_1 - v_2) dt} < M_3 \sqrt{\sum_{i=1}^{k_n} (c_{1i} - c_{2i})^2} < M_1 \|c_1 - c_2\|_1$$

Next since $x \mapsto \|x\| = \sqrt{\int_0^1 x^2(t)dt}$ and $x \mapsto \cos(x)$ are Lipschitz continuous, we have

$$|\cos \|v_1\| - \cos \|v_2\|| < M_2 \|\|v_1\| - \|v_2\|\| < M_1 \|c_1 - c_2\|_1 \quad (6.1)$$

Next note that $x \mapsto \sin(x)/x$ is Lipschitz continuous. Hence we have

$$\left\| \frac{\sin \|v_1\|}{\|v_1\|} - \frac{\sin \|v_2\|}{\|v_2\|} \right\| < M_2 \|\|v_1\| - \|v_2\|\| < M_1 \|c_1 - c_2\|_1 \quad (6.2)$$

Noting that

$$|q_1(t) - q_2(t)| < |\cos \|v_1\| - \cos \|v_2\|| + \left| \frac{\sin \|v_1\|}{\|v_1\|} v_1(t) - \frac{\sin \|v_2\|}{\|v_2\|} v_2(t) \right|$$

we have, combining equations 6.1 and 6.2,

$$\|q_1 - q_2\|_1 < M_1 \|c_1 - c_2\|_1 \quad (6.3)$$

Now consider $Q = q^2$. Observe that

$$\begin{aligned} (Q_1 - Q_2)(t) &= q_1^2(t) - q_2^2(t) = (q_1(t) - q_2(t))(q_1(t) + q_2(t)) \\ &= (\cos \|v_1\| + \cos \|v_2\| + \frac{\sin \|v_1\|}{\|v_1\|} v_1(t) + \frac{\sin \|v_2\|}{\|v_2\|} v_2(t))(q_1(t) - q_2(t)). \end{aligned}$$

Now $(\cos \|v_1\| + \cos \|v_2\| + \frac{\sin \|v_1\|}{\|v_1\|} v_1(t) + \frac{\sin \|v_2\|}{\|v_2\|} v_2(t))$ is a bounded function. Hence $\|Q_1 - Q_2\|_1 < M_1 \|c_1 - c_2\|_1$ using equation 6.3. Now we have $\gamma_i(t) = \int_0^t Q_i(u)du$, $t \in [0, 1]$, $i = 1, 2$. Then

$$|\gamma_1(t) - \gamma_2(t)| = \left| \int_0^t (Q_1(u) - Q_2(u))du \right| < \int_0^t |Q_1(u) - Q_2(u)|du \leq \|Q_1 - Q_2\|_1$$

Since f_p is Lipschitz continuous and strictly positive density on $[0, 1]$, we have

$$\|f_p(\gamma_1) - f_p(\gamma_2)\|_1 < M_4 \|\gamma_1 - \gamma_2\|_1$$

Consider $|f_1 - f_2| = |f_p(\gamma_1) \cdot \dot{\gamma}_1 - f_p(\gamma_2) \cdot \dot{\gamma}_2|$. Keeping in mind that $Q = \dot{\gamma}$, we have

$$\begin{aligned}
 |f_1(t) - f_2(t)| &= |f_p(\gamma_1(t)) \cdot Q_1(t) - f_p(\gamma_2(t)) \cdot Q_2(t)| \\
 &= |f_p(\gamma_1(t)) \cdot Q_1(t) - f_p(\gamma_2(t)) \cdot Q_1(t) + f_p(\gamma_2(t)) \cdot Q_1(t) - f_p(\gamma_2(t)) \cdot Q_2(t)| \\
 &\leq |Q_1(t)| M_1 \|\gamma_1 - \gamma_2\|_1 + |f_p(\gamma_2(t))| \|Q_1 - Q_2\|_1 \\
 &\leq M_2 \|\gamma_1 - \gamma_2\|_1 + M_3 \|\gamma_1 - \gamma_2\|_1 < M_0 \|c_1 - c_2\|_1.
 \end{aligned}$$

Therefore we have $|f_1 - f_2| < M_0 \|c_1 - c_2\|_1$ for some fixed $M_0 > 0$. \square

Remark 1: $H(f_1, f_2) < M_1 \sqrt{\|f_1 - f_2\|_1} < M_1 \sqrt{\|c_1 - c_2\|_1} < l_1 \sqrt{\|c_1 - c_2\|_\infty}$ for some fixed $l_1 > 0$ where $H(f_1, f_2)$ is the Hellinger metric between two densities f_1 and f_2 .

6.2 Proof of Lemma 1 and Corollary 1

Let us consider a fixed $f_0 = f_p(\Gamma(c_0)) \cdot \dot{\Gamma}(c_0)$. We note that $H(f_1, f_2) \leq l_1 \sqrt{\|c_1 - c_2\|_\infty}$ for some $l_1 > 0$ following the steps in section 6.1. So finding a δ covering for \mathcal{F}_n is equivalent to finding an $l_1 \sqrt{\delta}$ covering for the space of coefficients in the tangent space using L_∞ norm. Let us have a closer look at the space of coefficients. We have $\|v\| < \pi/4$ for tangent space representation of Γ , which is equivalent to $\|c\|_2 \leq l_3$, say. Therefore $\mathcal{F}_n \equiv \{c \in \mathbb{R}^{k_n} : \|c\|_2 \leq l_3\} = \mathcal{C}$, say. Then $\mathcal{C} \subset \{c \in \mathbb{R}^{k_n} : \|c\|_\infty \leq l_4\} \equiv \{c \in \mathbb{R}^{k_n} : |c_i| \leq l_4 \forall i = 1, \dots, k_n\} = \mathcal{C}_0$, say. Now \mathcal{C}_0 is a compact set with \mathcal{C} as a compact subset. Therefore the covering number N for \mathcal{C} would be less than the covering number for \mathcal{C}_0 . Since $\mathcal{C}_0 \equiv \{[-l_4, l_4]^{k_n}\}$, we have the covering number for \mathcal{C}_0 as $(\frac{2l_4}{l_1 \sqrt{\delta}})^{k_n}$. We obtain this by partitioning the interval $[-l_4, l_4]$ into pieces of length $l_1 \sqrt{\delta}$ for each coordinate so that the partition of \mathcal{C}_0 is reached through cross product. Then in each equivalent class of the partition of \mathcal{C}_0 we will have $\|c_1 - c_2\|_\infty \leq l_1 \sqrt{\delta}$ which is equivalent to $H(f_1, f_2) \leq \delta$. So we have the metric entropy for $\mathcal{F}_n = H(\cdot, \mathcal{F}_n) = H(u, \mathcal{F}_n) < k_n \log l/u$, where $l = 2l_4$ and $u = l_1 \sqrt{\delta}$. Now,

$$\int_{\epsilon^2/2^8}^{\sqrt{2}\epsilon} H^{1/2}\left(\frac{u}{l_3}, \mathcal{F}_n\right) du \leq \sqrt{k_n} \int \sqrt{\log(l_0/u)} du \leq \sqrt{k_n \log(M/\epsilon^2)} (\sqrt{2}\epsilon - \epsilon^2/256)$$

where $l_0 = l_3 l$ and $M = 2^8 l_0$. For the existence of an ϵ_n that satisfies Lemma 1 we need an ϵ_n less than 1 that satisfies

$$\sqrt{k_n \log(M/\epsilon^2)}(\sqrt{2}\epsilon - \epsilon^2/256) \leq C_4 n^{1/2} \epsilon^2 \quad (6.4)$$

But this inequality holds at 1– and hence there exists a smallest $\epsilon_n < 1$ that satisfies 6.4. The corollary follows directly from Theorem 1 in Wong and Shen [1995]

6.3 Proof of Lemma 2

Consider $\alpha = 1$ in (6.5). $\delta_n(1) = \inf_{f \in \mathcal{F}_n} \rho_1(p_0, f) = \inf_{f \in \mathcal{F}_n} \int p_0 g_1(p_0/f) = \inf_{f \in \mathcal{F}_n} \int \frac{(p_0-f)^2}{f}$. Let P_0 and F_p be the cdfs corresponding to the true density and the initial parametric estimate respectively. Then we have $\gamma_0 = F_p^{-1} \circ P_0$ has the tangent space representation v_0 obtained via exponential map of $\sqrt{\dot{\gamma}_0}$ satisfying $\|v_0\| < \pi/4$. This forces $\cos(\|v_0\|) + \frac{\sin(\|v_0\|)}{\|v_0\|} v_0$ to be always positive. Let f be the final density estimate and c_2 be the corresponding coefficient vector in the tangent space representation and v_1 be the corresponding element in the tangent space. Now we have $\|v_1\| < \pi/4$ corresponding to f because $c_2 \in V_\pi^{k_n}$ following the notation V_π^J introduced in Section 2 of the manuscript. That implies $\cos(\|v_1\|) + \frac{\sin(\|v_1\|)}{\|v_1\|} v_1 > 0$, i.e.

$$\dot{\gamma}(t) = \left(\cos(\|v_1\|) + \frac{\sin(\|v_1\|)}{\|v_1\|} v_1 \right)^2(t) > 0 \quad \forall t \in [0, 1]$$

Also $\dot{\gamma}(t)$ is continuous in t on a closed and bounded interval. So it attains its minima at some point t_0 such that $\dot{\gamma}(t) \geq \dot{\gamma}(t_0) > 0$ for all $t \in [0, 1]$. Thus it follows that $f(t) > M_1 \dot{\gamma}(t_0) = d$, say. Then we have, $\delta_n(1) = \inf_{f \in \mathcal{F}_n} \int \frac{(p_0-f)^2}{f} dt < \inf_{f \in \mathcal{F}_n} \|p_0 - f\|_\infty^2 / d = C_5 n^{\frac{-2\beta}{2\beta+1}}$ for some $C_5 > 0$.

6.4 Proof of Theorem 1

We have from equation 6.4 $\sqrt{k_n \log(M/\epsilon^2)}(\sqrt{2}\epsilon - \epsilon^2/256) < \sqrt{k_n \log(M/\epsilon^2)}\sqrt{2}\epsilon$. So for an upper bound of the smallest root we can solve the equation $\sqrt{k_n \log(M/\epsilon^2)}\sqrt{2}\epsilon = C_4 n^{1/2} \epsilon^2$. Let ϵ_n be of the form $\sqrt{M} n^{-\gamma} (\log n)^t$, $\gamma > 0$, and, let $k_n = n^\Delta$, $\Delta < 1$ Then $\log(M/\epsilon_n^2) = 2\gamma \log n - 2t \log \log n \leq 2\gamma \log n$.

So for an upper bound of the smallest root we can solve the equation

$$\sqrt{k_n 2^\gamma \log n} \sqrt{2} \epsilon = C_4 n^{1/2} \epsilon^2.$$

Therefore equating, $n^{\Delta/2} \sqrt{2^\gamma \log n} \sqrt{M} n^{-\gamma} (\log n)^t$ with $C_4 M n^{1/2} n^{-2\gamma} (\log n)^{2t}$, we get $\gamma = \frac{1}{2}(1 - \Delta)$, and $t = 1/2$. Thus we have $\epsilon_n = \sqrt{M} n^{\frac{-(1-\Delta)}{2}} \sqrt{\log n}$. We take Δ to be $\frac{1}{2\beta+1}$ to use the theoretical properties of Hölder space of order $\beta > 0$. Therefore $\epsilon_n = \sqrt{M} n^{\frac{\beta}{2\beta+1}} \sqrt{\log n}$ is an upper bound for the smallest value that satisfies the condition for Lemma 1. Therefore, using the definition given in Theorem 4 in Wong and Shen [1995], and using $\alpha = 1$, we get

$$\epsilon_n^* = \begin{cases} M n^{-\beta/(2\beta+1)} \sqrt{\log n}, & \text{if } \delta_n(1) < \frac{1}{4} C_1 M^2 n^{-2\beta/(2\beta+1)} \log n, \\ (4\delta_n(1)/C_1)^{1/2}, & \text{otherwise.} \end{cases}$$

But $\delta_n(1) = C_5 n^{-2\beta/(2\beta+1)} < \frac{1}{4} C_1 M^2 n^{-2\beta/(2\beta+1)} \log n$ for $n > \exp(4C_5/M^2 C_1)$. Thus for large enough n , $\epsilon_n^* = M n^{-\beta/(2\beta+1)} \sqrt{\log n}$ and following Theorem 4 of Wong and Shen [1995] we get

$$P(\|q^{1/2} - p_0^{1/2}\|_2 \geq \epsilon_n^*) \leq 5 \exp(-C_2 n (\epsilon_n^*)^2) + \exp(-\frac{1}{4} n \alpha C_1 (\epsilon_n^*)^2). \quad (6.5)$$

7. Estimation Algorithm

In this section we outline the estimation procedure and discuss some of the implementation issues. We discretize density functions using a dense uniform partition, $T = 100$ equidistant points over the interval $[0, 1]$. For approximating derivatives of a function, for example $\dot{\gamma}$ for a warping function γ , we use the first-order differences. The integrals are approximated using the trapezoidal method.

For optimizing log-likelihood function according to Equation 2.5 of the manuscript, we use the function *fminsearch* in MATLAB for our experiments. The *fminsearch* function uses a very efficient grid search technique to find the optimal values of coefficients $\{c_j\}$, corresponding to the chosen basis elements, to approximate the optimal warping function γ . However, *fminsearch* function can get stuck in locally-optimal solutions in some situations. To alleviate this problem we use an iterative, multi-resolution approach as follows. We start the optimization using a small number of basis elements J with $c = \mathbf{0}$, the point that maps to $\gamma_{id} \in \Gamma$ under H^{-1} . This implies

a low-resolution search and low-dimensional search space \mathbb{R}^J . Then, at each successive iteration we increase the resolution by increasing J and use the previous solution as the initial condition (with the additional components set to zero) for the next stage. This slow increase in J , while continually improving the optimal point c , performs much better in practice than using a large value of J directly in *fminsearch*.

Another important numerical issue is the final choice of J . For a fixed sample of size n , a large value of J may lead to overfitting and \hat{f} being a rough function. Also, a large value of J makes it harder for the search procedure to converge to an optimal solution. Efromovich [2010] and the references there in discusses different data-driven methods to choose the number of basis elements, by considering the number of basis elements itself as a parameter. We take a different data-driven approach for selecting the desired number of basis elements. Using a predetermined maximum number of basis points, we navigate through increasing number of basis elements and at each step, we compute the value of the Akaike’s Information Criterion (AIC) and choose the number of basis elements that results in the best value of the AIC, penalizing the number of basis functions used. We summarize the full procedure in **Algorithm 1**.

Algorithm 1 Improving solutions using *fminsearch* by tweaking the starting points

- i. Start with a low number of basis elements, say J
 - ii. Use $\mathbf{0}$ vector as the starting point and find the solution \mathbf{d} using *fminsearch*.
 - iii. Increase the number of basis elements, say J_1 more basis elements.
 - iv. Use $[\mathbf{0}, \mathbf{0}]$ and $[\mathbf{d}, \mathbf{0}]$ as two starting points. Compare the AIC for the two cases and choose the solution with better AIC value. Call the solution \mathbf{d} the optimal solution.
 - v. If the number of basis elements exceeds a predetermined large number, stop. Else go to step iii.
-

Experimental results show that Bayesian Information Criterion (BIC) overpenalizes the number of basis elements used and, therefore, some sharper features of the true density are lost in the estimate. So the experiments presented in the following sections use only the AIC penalty.

8. Simulation Studies

Next, we elaborate on the results from experiments on univariate unconditional density estimation procedure involving two simulated datasets, from Section 5 in the manuscript. The computations

described here are performed on an Intel(R) Core(TM) i7-3610QM CPU processor laptop, and the computational times are reported for each experiment. We compare the proposed solution with two standard techniques: (1) kernel density estimates with bandwidth selected by unbiased cross validation method, henceforth referred to as *kernel(ucv)*, (2) a standard Bayesian technique using the function *DPdensity* in the R package *DPPackage*. The Bayesian approach naturally has a longer run-time. For both the simulated examples, we use 2000 MCMC runs with 500 iterations as burn in period for the Bayesian technique. We compare the methods both in terms of numerical performance and computational cost. Here we illustrate the performance of the various methods using a representative simulation. We highlight the performance improvement over an (misspecified) initial parametric and nonparametric density estimate brought about by warping. For the initial parametric estimate we have chosen a normal density truncated to $[0, 1]$ with mean and standard deviation estimated from the sample. For the initial nonparametric estimate, we used inbuilt MATLAB function *ksdensity*.

8.1 Example 1

We borrow the first example from Tokdar [2007] and Lenk [1991], where $p_0 \propto 0.75\exp(\text{rate} = 3) + 0.25\mathcal{N}(0.75, 2^2)$, a mixture of exponential and normal density truncated to the interval $[0, 1]$: We generate $n = 100$ observations to study estimation performance. Here we use Meyer wavelets as the basis set for the tangent space representation of γ s. We use an ad hoc choice of $J = 15$ basis elements to approximate the tangent space. Also, we use an unpenalized log likelihood for optimization.

Figure 7 (left panel) shows a substantial improvement in the final warped estimate over the initial parametric estimate. Incidentally, it also does a better job in capturing the left peak as compared to the *kernel(ucv)* method. Standard kernel methods need additional boundary correction techniques to be able to capture the density at the boundaries, as studied in Karunamuni and Zhang [2008] and the references therein. However the warped density seems to perform better estimation near the boundaries compared to the other techniques. The right panel displays the warped result when using *ksdensity* output as the initial estimate. It also provides solutions obtained using

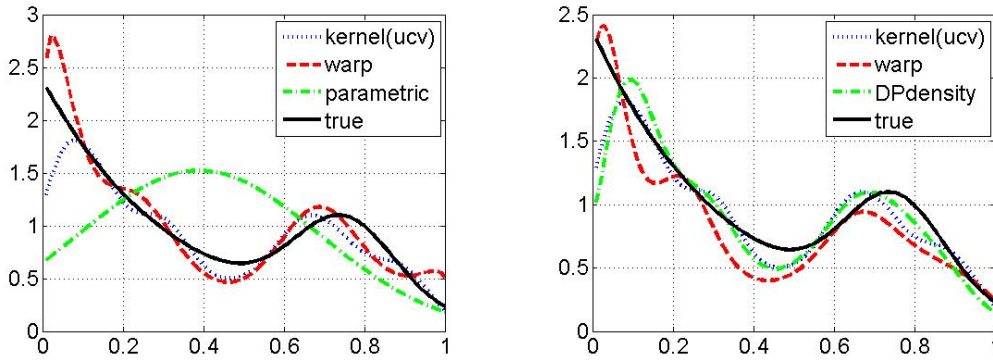


Figure 7: The left panel compares the warped estimate \hat{f} with other estimates when f_p is parametric. The middle panel shows the corresponding evolution of the negative of log-likelihood function during optimization. The right figure compares the warped estimate with others when f_p is ksdensity.

$kernel(ucv)$ and $DPdensity$. Once again, this warped estimate provides a substantial improvement over the initial solution.

8.2 Example 2

For the second example we take Example 10 from Marron and Wand [1992], which uses a claw density: $p_0 = \frac{1}{2}\mathcal{N}(0, 1) + \sum_{l=0}^4 \frac{1}{10}\mathcal{N}(\frac{l}{2} - 1, (0.1)^2)$. We estimate the domain boundaries and

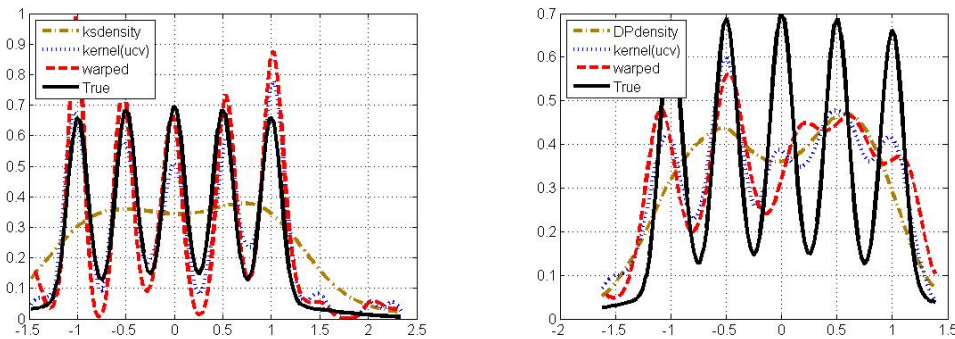


Figure 8: The left panel shows the improvement over initial ksdensity estimate. Both $kernel(ucv)$ and warped estimate have a good performance here. The right panel shows that all the methods fail to capture all the peaks. $Kernel(ucv)$ performance is very similar to the warped estimate.

unlike the previous example, instead of fixing the number of tangent basis elements, we employ

Algorithm 1 described in Section 7 to find the optimal number of basis elements based on the AIC, with a maximum allowed value of 40 basis elements. Consequently, the computation cost goes up.

Acknowledgements

This research was supported in part by the NSF grants to AS – NSF DMS CDS&E 1621787 and NSF CCF 1617397.

References

- Ian S Abramson. On bandwidth variation in kernel estimates-a square root law. *The annals of Statistics*, pages 1217–1223, 1982.
- David M Bashtannyk and Rob J Hyndman. Bandwidth selection for kernel conditional density estimation. *Computational Statistics & Data Analysis*, 36(3):279–298, 2001.
- A Bhattacharya, D Pati, and DB Dunson. Latent factor density regression models. *Biometrika*, 97(1):1–7, 2010.
- Lucien Birgé, Pascal Massart, et al. Minimum contrast estimators on sieves: exponential bounds and rates of convergence. *Bernoulli*, 4(3):329–375, 1998.
- Yeonseung Chung and David B. Dunson. Nonparametric bayes conditional distribution modeling with variable selection. *Journal of the American Statistical Association*, 104(488):1646–1660, 2009. URL <http://pubs.amstat.org/doi/abs/10.1198/jasa.2009.tm08302>.
- Miguel De Carvalho. Confidence intervals for the minimum of a function using extreme value statistics. *International Journal of Mathematical Modelling and Numerical Optimisation*, 2(3):288–296, 2011.
- Maria De Iorio, Peter Muller, Gary L. Rosner, and Steven N. MacEachern. An anova model for dependent random measures. *Journal of the American Statistical Association*, 99(465):205–215, 2004. URL <http://www.jstor.org/stable/27590366>.
- David L Donoho, Iain M Johnstone, Gérard Kerkycharian, and Dominique Picard. Density estimation by wavelet thresholding. *The Annals of Statistics*, pages 508–539, 1996.
- Hassan Doosti and Peter Hall. Making a non-parametric density estimator more attractive, and more accurate, by data perturbation. *Journal of the Royal Statistical Society: Series B (Statistical Methodology)*, 78(2):445–462, 2016.
- David B Dunson and Ju-Hyun Park. Kernel stick-breaking processes. *Biometrika*, 95(2):307–323, 2008.

- David B. Dunson, Natesh Pillai, and Ju-Hyun Park. Bayesian density regression. *Journal of the Royal Statistical Society. Series B (Statistical Methodology)*, 69(2):pp. 163–183, 2007. ISSN 13697412. URL <http://www.jstor.org/stable/4623261>.
- Sam Efromovich. Orthogonal series density estimation. *Wiley Interdisciplinary Reviews: Computational Statistics*, 2(4):467–476, 2010.
- Michael D Escobar and Mike West. Bayesian density estimation and inference using mixtures. *Journal of the american statistical association*, 90(430):577–588, 1995.
- J. E Griffin and M. F. J Steel. Order-based dependent dirichlet processes. *Journal of the American Statistical Association*, 101(473):179–194, 2006. URL <http://pubs.amstat.org/doi/abs/10.1198/016214505000000727>.
- Peter Hall, Simon J Sheather, MC Jones, and James Stephen Marron. On optimal data-based bandwidth selection in kernel density estimation. *Biometrika*, 78(2):263–269, 1991.
- Bruce E Hansen. Nonparametric conditional density estimation. *Unpublished manuscript*, 2004.
- Nils Lid Hjort and Ingrid K Glad. Nonparametric density estimation with a parametric start. *The Annals of Statistics*, pages 882–904, 1995.
- Torsten Hothorn, Lisa Möst, and Peter Bühlmann. Most likely transformations. *arXiv preprint arXiv:1508.06749*, 2015.
- Sonia Jain and Radford M Neal. A split-merge markov chain monte carlo procedure for the dirichlet process mixture model. *Journal of Computational and Graphical Statistics*, 2012.
- Maria Kalli, Jim E Griffin, and Stephen G Walker. Slice sampling mixture models. *Statistics and computing*, 21(1):93–105, 2011.
- Rhoana J Karunamuni and Shunpu Zhang. Some improvements on a boundary corrected kernel density estimator. *Statistics & Probability Letters*, 78(5):499–507, 2008.
- Suprateek Kundu and David B Dunson. Latent factor models for density estimation. *Biometrika*, 101(3):641–654, 2014.
- Serge Lang. *Fundamentals of differential geometry*, volume 191. Springer Science & Business Media, 2012.
- Peter J Lenk. The logistic normal distribution for bayesian, nonparametric, predictive densities. *Journal of the American Statistical Association*, 83(402):509–516, 1988.
- Peter J Lenk. Towards a practicable bayesian nonparametric density estimator. *Biometrika*, 78(3):531–543, 1991.
- Tom Leonard. Density estimation, stochastic processes and prior information. *Journal of the Royal Statistical Society. Series B*

- (*Methodological*), pages 113–146, 1978.
- Oleg Lepski. Adaptive estimation over anisotropic functional classes via oracle approach. *The Annals of Statistics*, 43(3):1178–1242, 2015.
- Qi Li and Jeffrey Scott Racine. *Nonparametric econometrics: theory and practice*. Princeton University Press, 2007.
- Matthew P Longnecker, Mark A Klebanoff, Haibo Zhou, and John W Brock. Association between maternal serum concentration of the ddt metabolite dde and preterm and small-for-gestational-age babies at birth. *The Lancet*, 358(9276):110–114, 2001.
- Steven N. MacEachern. Dependent nonparametric processes. *ASA Proceedings of the Section on Bayesian Statistical Science*, 1999. URL <http://aima.eecs.berkeley.edu/~russell/classes/cs294/f05/papers/maceachern-1999.pdf>.
- Steven N MacEachern and Peter Müller. Estimating mixture of dirichlet process models. *Journal of Computational and Graphical Statistics*, 7(2):223–238, 1998.
- J Steve Marron and Matt P Wand. Exact mean integrated squared error. *The Annals of Statistics*, pages 712–736, 1992.
- Peter Müller, Alaattin Erkanli, and MIKE West. Bayesian curve fitting using multivariate normal mixtures. *Biometrika*, 83(1):67–79, 1996.
- Andriy Norets and Justinas Pelenis. Bayesian modeling of joint and conditional distributions. *Journal of Econometrics*, 168:332–346, 2012.
- Murray Rosenblatt. Remarks on some nonparametric estimates of a density function. *The Annals of Mathematical Statistics*, 27(3):832–837, 1956.
- S Saoudi, A Hillion, and F Ghorbel. Non-parametric probability density function estimation on a bounded support: Applications to shape classification and speech coding. *Applied Stochastic models and data analysis*, 10(3):215–231, 1994.
- S Saoudi, F Ghorbel, and A Hillion. Some statistical properties of the kernel-diffeomorphism estimator. *Applied stochastic models and data analysis*, 13(1):39–58, 1997.
- Simon J Sheather and Michael C Jones. A reliable data-based bandwidth selection method for kernel density estimation. *Journal of the Royal Statistical Society. Series B (Methodological)*, pages 683–690, 1991.
- Anuj Srivastava and Eric P Klassen. *Functional and shape data analysis*. Springer, 2016.
- EG Tabak and Cristina V Turner. A family of nonparametric density estimation algorithms. *Communications on Pure and Applied*

Mathematics, 66(2):145–164, 2013.

Esteban G Tabak and Giulio Trigila. Data-driven optimal transport. *Commun. Pure. Appl. Math. doi*, 10:1002, 2014.

George R Terrell and David W Scott. Variable kernel density estimation. *The Annals of Statistics*, pages 1236–1265, 1992.

Surya T Tokdar. Towards a faster implementation of density estimation with logistic gaussian process priors. *Journal of Computational and Graphical Statistics*, 16(3):633–655, 2007.

Surya T Tokdar, Yu M Zhu, Jayanta K Ghosh, et al. Bayesian density regression with logistic gaussian process and subspace projection. *Bayesian analysis*, 5(2):319–344, 2010.

Hans Triebel. Theory of function spaces. iii, volume 100 of monographs in mathematics. *BirkhauserVerlag, Basel*, 2006.

Bradley C Turnbull and Sujit K Ghosh. Unimodal density estimation using bernstein polynomials. *Computational Statistics & Data Analysis*, 72:13–29, 2014.

Philippe Van Kerm. Adaptive kernel density estimation. *Stata Journal*, 3(2):148–156, 2003.

V Vermehren and HM de Oliveira. Close expressions for meyer wavelet and scale function. *arXiv preprint arXiv:1502.00161*, 2015.

Wing Hung Wong and Xiaotong Shen. Probability inequalities for likelihood ratios and convergence rates of sieve mles. *The Annals of Statistics*, pages 339–362, 1995.

Florida State University

E-mail: (s.dasgupta@stat.fsu.edu)

Texas A&M University

E-mail: (debdeep@stat.tamu.edu)

Florida State University

E-mail: (anuj@stat.fsu.edu)